ELSEVIER

International Journal of Adhesion & Adhesives 27 (2007) 636–646

International Journal of Adhesion & Adhesives

www.elsevier.com/locate/ijadhadh

Modelling non-linear creep behaviour of an epoxy adhesive

G. Dean*

Engineering and Process Control Division, National Physical Laboratory, Teddington, Middlesex, TW11 0LW, UK

Accepted 20 November 2006
Available online 29 December 2006

Abstract

The creep behaviour of a rubber-toughened, two-part epoxy adhesive has been measured using specimens that have been stored in a desiccator and under ambient humidity. Tensile and compressive creep compliance curves for the dry material have been modelled using a stretched exponential function with parameters representing the short-term compliance, a mean retardation time for the relaxation process and a distribution of retardation times for the process. This function shows small departures from data at high stresses or long times. The retardation time parameter is observed to be dependent upon the magnitude of the stress giving rise to non-linear behaviour and enhanced creep deformation at moderate stress levels. At stress levels where behaviour is non-linear, creep curves under a uniaxial compressive stress are different from results measured under tension at the same stress. This is interpreted by relating the mean retardation time to an effective stress which is dependent upon the magnitudes of the shear and hydrostatic components of the applied stress.

Results for material that has been stored under ambient humidity show a significantly higher creep rate than observed for the dry material. These results cannot be modelled using the function applied to the results for dry material. Attempts have been made to describe the creep behaviour of the adhesive with absorbed water in terms of two, overlapping relaxation processes such that the contribution from the short-term process is sensitive to the concentration of absorbed water. The creep results for the dry material have also been analysed using this two-process model with a smaller contribution from the short-term process, and this has produced a better description of behaviour at high stresses and long times than obtained with the function that models only a single process.

Keywords: Epoxy/epoxides; Creep/mechanical relaxation; Viscoelasticity; Non-linear deformation

1. Introduction

Epoxy resins have been developed as structural adhesives where they are usually blended with rubbers to increase their ductility. They are tough, engineering materials that are widely used in applications where they are required to support significant levels of stress. In these applications, a knowledge of the stress and strain distributions in the adhesive is required to assist competent design of a bonded product. A finite element analysis can be used to calculate these distributions, and the results of an analysis can enable variations in the design of a component to be explored in order to reduce stress or strain levels in regions of stress concentration in the adhesive layer. In conjunction with a valid failure criterion for the polymer, it should be possible to decide safe working limits for the component.

Confidence in predictions from these analyses requires the use of models that accurately describe the deformation behaviour of the polymer as well as accurate and relevant materials property data. Whilst epoxy adhesives are usually highly cross-linked polymers with a glass transition temperature well above ambient temperatures, they still exhibit viscoelastic behaviour [1–4]. Properties will therefore vary with time under load, especially at elevated stresses. Under long-term loading, properties will decrease progressively with time, and stress and strain levels in the adhesive will be very different from values calculated using property data obtained from tests of short duration. In particular, if deformation behaviour is non-linear then this will give rise to a redistribution of stress and strain with strain levels increasing more rapidly than expected from a linear analysis.

*Tel.: +44 208 943 6779; fax: +44 208 614 0427.
E-mail address: greg.dean@npl.co.uk.

0143-7496/$ - see front matter
doi:10.1016/j.ijadhadh.2006.11.004

Short-term tests on epoxies reveal that deformation behaviour is, to a good approximation, linear up to moderate stress levels, which are in the region of half the peak or flow stress [5]. With increasing time under load, the stiffness of the material not only decreases with time but the rate of decrease increases with stress giving rise to significant non-linear behaviour [6]. Materials models for non-linear creep that are currently available in finite element packages have been developed to describe time-dependent deformation arising from plastic flow. These models are not able to describe the deformation behaviour of plastics which results from viscoelastic relaxation processes in the molecular network of these materials. Creep models for polymeric materials in finite element systems approximate the material as a series of elastic springs and viscous elements. The simplest viscoelastic models are those of Maxwell (spring and dashpot in series) and Kelvin (spring and dashpot in parallel). The standard model consists of a spring that is in series with a second spring and a viscous element that are in parallel, as shown in Fig. 1.

When the standard model is subjected to a constant stress σ_0, the time-varying strain is given by

$$\varepsilon(t) = \varepsilon_0 + \Delta\varepsilon(1 - \exp - (t/\tau_0)), \quad (1)$$

where ε_0 is the strain across the spring E_0 and $\Delta\varepsilon$ is the relaxed strain across the parallel spring and viscous element after a sufficient period of time for completion of the relaxation process (and hence the flow of the viscous element). The parameter τ_0 is the creep retardation time for the relaxation process in the model shown in Fig. 1 and is given by the ratio of the viscosity η of the viscous element to the spring stiffness E. The single retardation time process given by Fig. 1 will not model creep behaviour in real polymers where relaxation mechanisms span a wide range of retardation times. In order to accommodate the wide distribution of relaxation times that occur in polymer relaxation processes, several of these elements are required with different spring stiffnesses and dashpot viscosities. Even then, such models will only describe linear creep or stress relaxation behaviour unless additional functions are included to represent the viscous elements with stress-dependent viscosities. A related description of creep deformation, which requires the inclusion of far fewer model parameters, involves a modification to Eq. (1) as follows:

$$\varepsilon(t) = \varepsilon_0 + \Delta\varepsilon(1 - \exp - (t/\tau)^n). \quad (2)$$

Here, τ is a mean, or effective, retardation time and n is a parameter which is less than unity and will broaden the timescale over which the strain will increase with creep time. Whilst this is a versatile function, the assumptions associated with the introduction of the single parameter n to represent a distribution of retardation times imply that the function is not expected to model creep behaviour accurately over the whole of the relaxation process.

From Eq. (2), a creep compliance function $D(t)$ can be defined which is a material property that characterises creep behaviour so that

$$D(t) = \varepsilon(t)/\sigma_0 = D_0 + \Delta D(1 - \exp - (t/\tau)^n), \quad (3)$$

where D_0 is the instantaneous compliance of the material and ΔD is the magnitude of the change in compliance with creep time. This function has been used to model relaxation phenomena and creep deformation in a variety of polymers [7,8] and is particularly useful for those situations where the experimental creep time is a significant fraction of the time spanned by the relaxation process [9].

The main mechanism responsible for creep in glassy polymers, such as epoxies at ambient temperatures, is the glass-to-rubber relaxation mechanism. The time scale for this mechanism spans many decades of time. For structural epoxies where the glass transition temperature T_g is well above operating temperatures, it is only the short-time tail of the mechanism that contributes to creep behaviour even for extended periods under load. Under these circumstances, an alternative creep function of the following form can be more applicable [10,11]

$$D(t) = D_0 \exp(t/t_0)^m. \quad (4)$$

The parameter m characterises a broad spectrum of retardation times whose mean value is now t_0.

For a model to be used in a creep stress analysis, it must be able to describe creep behaviour in the non-linear region of stress and under multiaxial stress states. The extension of Eq. (4) for this purpose is explained in Section 3 using the results of measurements made on a two-part epoxy adhesive.

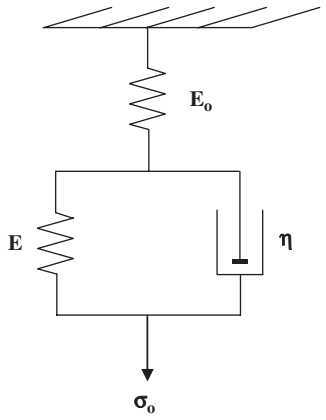

Fig. 1. A simple model for creep in a linear viscoelastic material.

2. Material

Creep studies have been carried out under uniaxial tensile and uniaxial compressive stresses on a two-part epoxy adhesive supplied by 3 M Ltd with the designation DP460. The mixed resin was cast into a plate mould with lateral dimensions 250 mm by 200 mm and with a uniform thickness of 3.2 mm. The moulding was allowed to cure at 23 °C for a period of 24 h and was then post-cured at

100 °C for 30 min. Standard tensile specimens as specified in ISO 3167 were machined from the mouldings for the measurement of creep deformation under uniaxial tension. Contacting extensometers were used for the measurement of creep strain. For compression tests, specimens were approximately 10 mm × 10 mm, and care was taken in the machining of edge faces to ensure that opposite faces were as parallel as possible. Specimens were loaded between platens in a universal testing machine under load control. The faces of the platens were polished and set up using an alignment fixture on one platen so that faces were accurately parallel. The change in platen separation during a compressive creep test was measured using three displacement transducers equally spaced around the circumference of the platens.

Two series of specimens were prepared from separate batches of the adhesive. With the first series, specimens were stored in a desiccator for a period of 3 months prior to creep testing. This period of storage was chosen to minimise any effect of physical ageing on creep behaviour [8–11]. The second series of specimens was stored in a laboratory under ambient humidity. These specimens absorbed moisture from the atmosphere, and the water content was 0.8% by weight at the start of the creep tests.

3. Modelling non-linear creep in the dry adhesive

3.1. Non-linear behaviour

Fig. 2 shows measured curves of the tensile creep compliance $D(t)$ against $\log_{10}$ time for specimens of the epoxy adhesive that were stored in a desiccator for 3 months prior to testing. Results are shown of measurements under different levels of stress. Creep behaviour is seen to depend on the magnitude of the stress for stress levels above about 10 MPa and to shift to shorter times with little apparent change of shape. This suggests that if Eq. (4) is used to model these curves then t_0 is the only parameter to change significantly with stress, as observed by other workers [12,13]. This is illustrated by the continuous lines that are plotted with each curve which are best fits to the data obtained using Eq. (4) with the values for the parameters for each fit listed in Table 1.

It can be seen that a very good fit is obtained to measured data for compliance values up to about 0.9 GPa^{-1}. Measured compliances then fall slightly below the best fit using Eq. (4) for stresses between 20 and 25.5 MPa whilst at 30 MPa measured values are higher than the equation. These departures of measured values from model predictions using Eq. (4) may be due to small changes in the parameters m and t_0 over extended periods of creep time or a dependence of m on stress. This issue will be addressed further in Section 4 of this paper, but it may be worth noting here that the fits to data in Fig. 2 could be improved at longer creep times by choice of slightly different values for t_0 which would accordingly lower the quality of the fit at shorter times.

Table 1
Values for the parameters in Eq. (4) used to obtain the fits to data in Fig. 2

σ_0 (MPa)	D_0 (GPa^{-1})	m	t_0 (s)
5	0.435	0.33	3.0×10^7
10	0.435	0.33	1.6×10^7
20	0.44	0.33	3.0×10^6
25	0.445	0.33	7.3×10^5
25.5	0.45	0.33	5.5×10^5
30	0.45	0.33	1.3×10^5

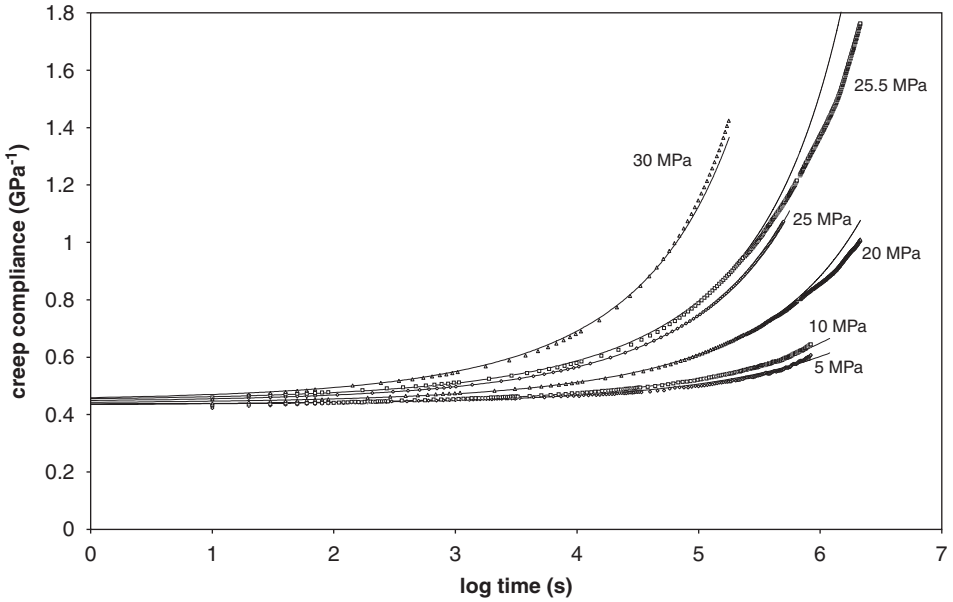

Fig. 2. Creep compliance curves measured on dry specimens of the epoxy adhesive at different stresses. The continuous lines are best fits to the data using Eq. (4).

Reference to the values in Table 1 reveals that, to a good approximation, the parameters D_0 and m are independent of stress, and the origin of non-linear behaviour is caused by a reduction in the mean retardation time parameter t_0 with increasing stress leading to a progressive shift of curves to shorter creep times. This reduction in t_0 and hence increase in molecular mobility brought about by elevated stresses is consistent with the Eyring model for plastic flow [14,15]. In this model, the molecular motions associated with flow are represented by thermally activated transitions across an energy barrier separating two different molecular conformations. It is proposed that the application of stress changes the barrier height leading to an increase in the rate of transitions across the barrier in one direction and a resultant increase in the population of conformational states with the lower energy and an associated increase in extension with time. The associated strain rate $\dot{\varepsilon}$ is then predicted by the model to be given by

$$\dot{\varepsilon} = \dot{\varepsilon}_0 \sinh(c\,\sigma), \tag{5}$$

where $\dot{\varepsilon}_0$ and c are functions of temperature and other parameters in the model. The spring and viscous element models of viscoelastic behaviour, such as that illustrated in Fig. 1, relate the retardation time parameter t_0 (or more strictly its use as a relaxation time parameter in a stress relaxation function) to spring and viscosity properties E and η, respectively, by the equation

$$t_0 = \frac{\eta}{E} = \frac{\sigma}{\dot{\varepsilon}E}. \tag{6}$$

Combining this with Eq. (5) leads to the following relationship between t_0 and the applied stress

$$t_0 = \frac{C\sigma}{\sinh(c\,\sigma)}, \tag{7}$$

where C is a new parameter.

Attempts to relate the values for the parameter t_0 in Table 1 to the creep stress σ_0 using Eq. (7) were not very successful. It was found that a better description could be obtained by the empirical relationship [13]

$$t_0 = A\exp-(\alpha\sigma_0^2). \tag{8}$$

This is illustrated by the plot of $\log_e t_0$ against σ_0^2 in Fig. 3 which gives values for $A = 3.3 \times 10^7$ s and $\alpha = 0.0062$ MPa^{-2}.

Eq. (8) implies a dependence of t_0 upon stress at all stress levels and therefore no limiting stress below which behaviour is linear. However, at stress levels below 10 MPa the form of Eq. (8) gives only a small change in t_0 with stress leading to essentially linear creep behaviour when used with the creep function in Eq. (4).

3.2. Extension to creep under multiaxial stress

Fig. 4 compares creep compliance curves for the adhesive measured under uniaxial tensile and uniaxial compressive stresses of 25 MPa. Also shown for reference is the tensile curve at a low stress, where behaviour is linear, calculated using Eq. (4) with values for D_0 and m obtained from Table 1 and t_0 from Eq. (8). At low stresses, compliance curves in tension and compression are expected to be the same. Under higher stresses, where behaviour is non-linear, the results in Fig. 4 show that the reduction in t_0 is less under compression than under tension. The magnitude of t_0 is determined, therefore, by the stress state as well as its magnitude. It is possible to incorporate this observation into the model by invoking that t_0 is determined by the magnitude of an effective stress $\bar{\sigma}$ that is a function of the shear component of applied stress as well as the hydrostatic component. This is analogous to the

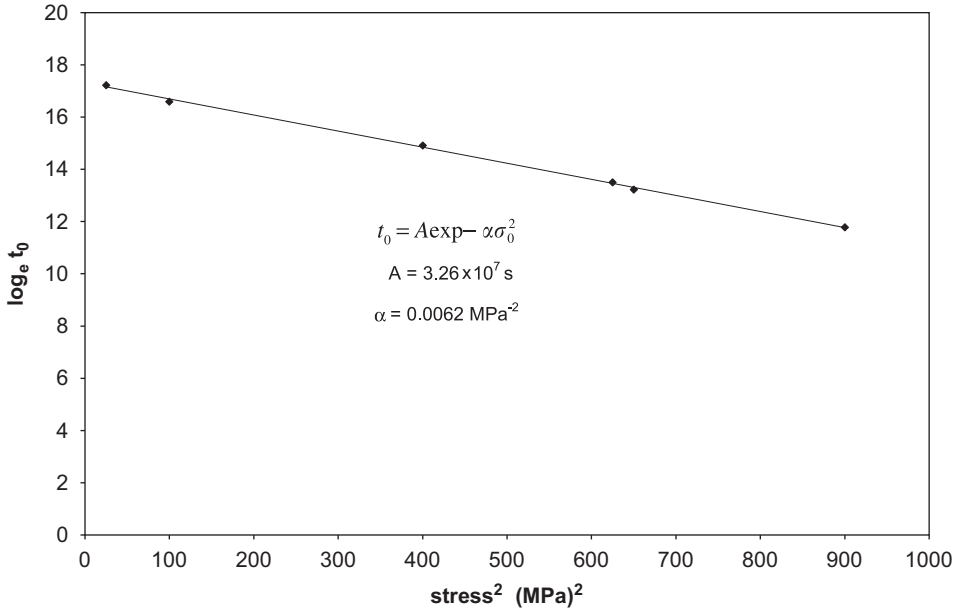

Fig. 3. Plot of $\log_e$ of the retardation times t_0 for the creep curves in Fig. 2 against the square of the creep stress (see Table 1).

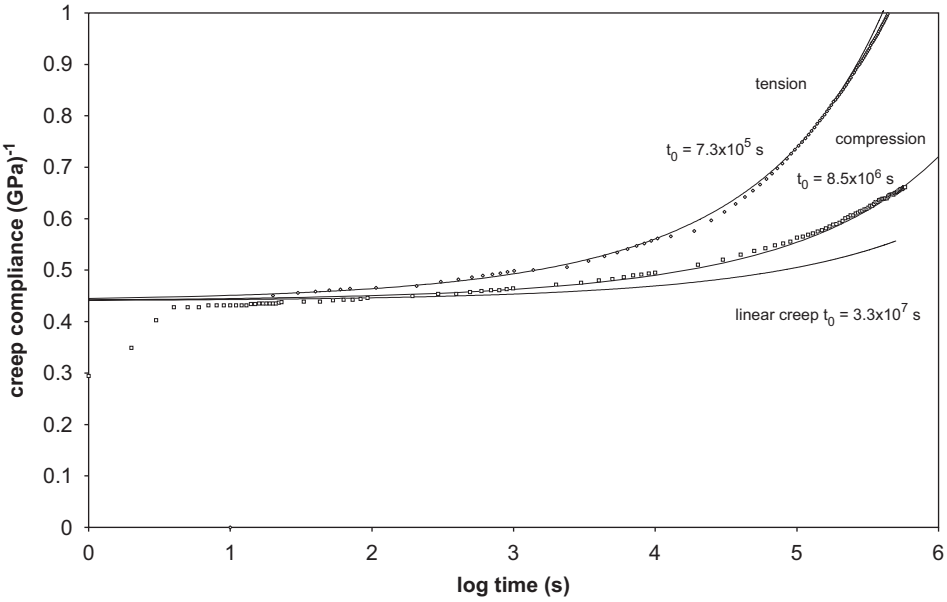

Fig. 4. Measured creep curves under tension and compression at a stress of 25 MPa modelled using Eq. (4). Also shown is the predicted curve for linear creep based on the data in Fig. 3 and Table 1.

formulation of most yield criteria for plastics. By analogy with the linear Drucker–Prager yield criterion, which has sensitivity to hydrostatic stress [16,17], it is proposed that the effective stress $\bar{\sigma}$ is a linear sum of contributions from the shear and hydrostatic components of stress

$$\bar{\sigma} = \frac{(\lambda+1)}{2\lambda}\sigma_e + \frac{3(\lambda-1)}{2\lambda}\sigma_m. \tag{9}$$

Here σ_e and σ_m are the effective shear and the hydrostatic components of the creep stress, respectively, and are given in terms of principal components of a multiaxial stress σ_1, σ_2 and σ_3 by

$$\sigma_e = [\tfrac{1}{2}[(\sigma_1-\sigma_2)^2 + (\sigma_2-\sigma_3)^2 + (\sigma_1-\sigma_3)^2]]^{1/2} \tag{10}$$

and

$$\sigma_m = \tfrac{1}{3}(\sigma_1+\sigma_2+\sigma_3). \tag{11}$$

The parameter λ is a measure of the sensitivity of the retardation time t_0 to the hydrostatic component of stress. Under a uniaxial tensile stress σ_0, $\bar{\sigma} = \sigma_0$, and under a compressive stress σ_c, $\bar{\sigma} = \sigma_c/\lambda$. So Eq. (8) remains valid under tension whilst under compression

$$t_0 = A\exp -\frac{\alpha}{\lambda^2}\sigma_c^2. \tag{12}$$

Using Eq. (4) to model the compressive data in Fig. 4 gives a value for $t_0 = 8.5\times10^6$ s under a compressive stress $\sigma_c = 25$ MPa. Using the values for A and α from tensile data in Fig. 3 with Eq. (12) gives a value for $\lambda = 1.7$ for this epoxy adhesive.

4. Modelling creep behaviour of the adhesive with absorbed water

4.1. Non-linear behaviour

Fig. 5 shows measured creep compliance curves at different stress levels for specimens that have been stored under ambient humidity for 8 weeks prior to loading. Measurements of changes in the mass of each specimen with storage time showed that the increase in the water content of the specimens over this period was 0.8% by mass. Attempts to model the data using Eq. (4) with the same value for $m = 0.33$ are shown by the continuous lines with each test. Values for the parameters are given in Table 2.

The values for the retardation time parameter t_0 are much lower than values shown in Table 1 for the dry material at the same stress showing that the specimens with absorbed water are creeping significantly faster at short times. However, the departures of measured values from Eq. (4) show that the model is breaking down at relatively short creep times in the case of material with absorbed water. One explanation for this might be that the presence of water in the adhesive is broadening the distribution of retardation times as well as reducing them. To explore this possibility, new fits to the data in Fig. 5 were attempted with lower values for the parameter m as shown in Fig. 6 using a value for $m = 0.18$. Whilst a better fit to data can be obtained at long times, the quality of the fit at short and intermediate times is totally inadequate.

The shape of the creep curves in Fig. 5 at low and intermediate stresses suggest that the creep deformation is actually composed of contributions from two relaxation processes. At long creep times there is a contribution from

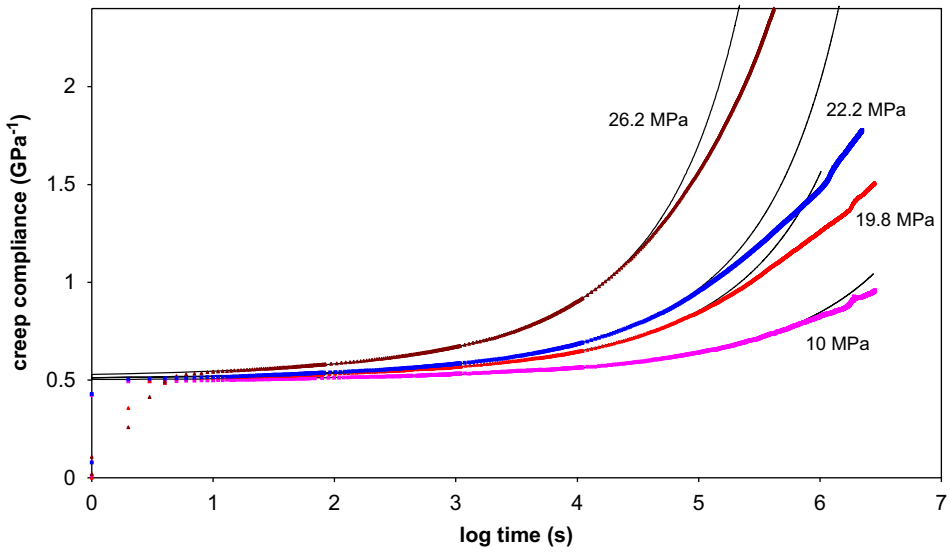

Fig. 5. Creep curves for the epoxy adhesive stored under ambient humidity. The continuous lines are best fits to the data using Eq. (4) with $m = 0.33$.

Table 2
Values for the parameters in Eq. (4) used to obtain the fits to data in Fig. 5

σ_0 (MPa)	D_0 (GPa^{-1})	m	t_0 (s)
9.9	0.5	0.33	7.0×10^6
19.8	0.505	0.33	7.0×10^5
22.2	0.505	0.33	3.7×10^5
26.2	0.515	0.33	5.8×10^4

the glass-to-rubber relaxation mechanism, but, at short creep times, the deformation is dominated by a contribution from another mechanism whose magnitude might be sensitive to the concentration of water in the adhesive. The presence of a small relaxation process whose magnitude is sensitive to water content has been reported in the literature in certain epoxy resin systems using dynamic mechanical measurements over a range of temperature [18,19]. The process is referred to as the ω-relaxation and lies in the temperature range between 20 and 80 °C depending on the chemistry of the epoxy. Dynamic mechanical measurements comparing results for specimens stored dry and under ambient humidity for the DP 460 epoxy studied here are shown in Fig. 7. These results reveal that the glass transition temperature has been reduced from a value of about 80 °C for the dry material to a value of about 75 °C with absorbed water (based on the shift in the peak of the loss modulus). There is no clear evidence, however, of the presence of a relaxation mechanism in the specimen with absorbed water at a temperature below 50 °C although it is possible that evidence for a small peak in loss modulus might be lost by overlap with the low temperature tail of the α-mechanism associated with the glass-to-rubber transition.

In order to explore the possibility of two relaxation mechanisms contributing to the creep deformation of the epoxy with absorbed water, we proceed by observing that the mean retardation time for the short-time process will be comparable with creep times. Under these circumstances, it will not be possible to use Eq. (4) to model the creep deformation since this function is only suitable for describing deformation arising from the short-time tail of a relaxation process (see Section 1). The creep function given by Eq. (3) is more suitable. In this equation, D_0 is the creep compliance at very short times and ΔD is the amplitude of the short-time process. The dynamic storage modulus results for specimens with absorbed water show some evidence for a possible relaxation process in the temperature range between 40 and 80 °C with an unrelaxed (low temperature) modulus limit E_U of around 2 GPa and a relaxed (high temperature) limit E_R of around 1 GPa. An estimate of the compliance amplitude of the process then follows from the relationship

$$\Delta D = \frac{1}{E_R} - \frac{1}{E_U} = \frac{E_U - E_R}{E_U E_R}. \tag{13}$$

This suggests a value for ΔD in the region of 1 GPa^{-1}. In accordance with results reported earlier in this paper on dry material, values for the retardation time, τ, for this short-time process would be expected to decrease with stress. The contribution to creep behaviour from the longer term α-mechanism associated with the glass-to-rubber transition can be described by Eq. (4) since retardation times will be larger than creep times. However, since the deformations arising from the two processes overlap in time, the short-time compliance D_0 in Eq. (4) must be replaced by the compliance level attained by the short-time mechanism. The compliance function for the two-process model is therefore

$$D(t) = (D_0 + \Delta D(1 - \exp - (t/\tau)^n)) \exp(t/t_0)^m. \tag{14}$$

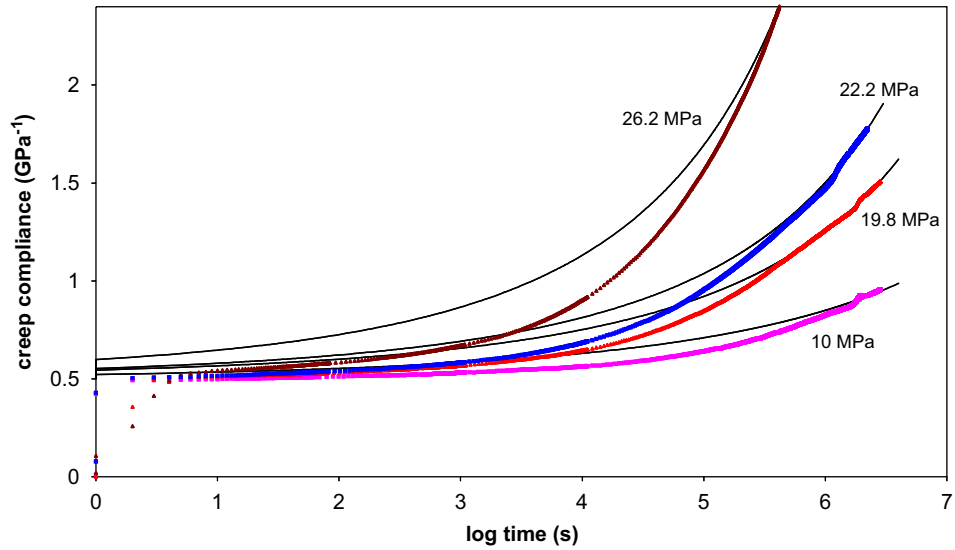

Fig. 6. Comparison of the creep data for specimens stored under ambient humidity with predictions using Eq. (4) with a value for $m = 0.18$.

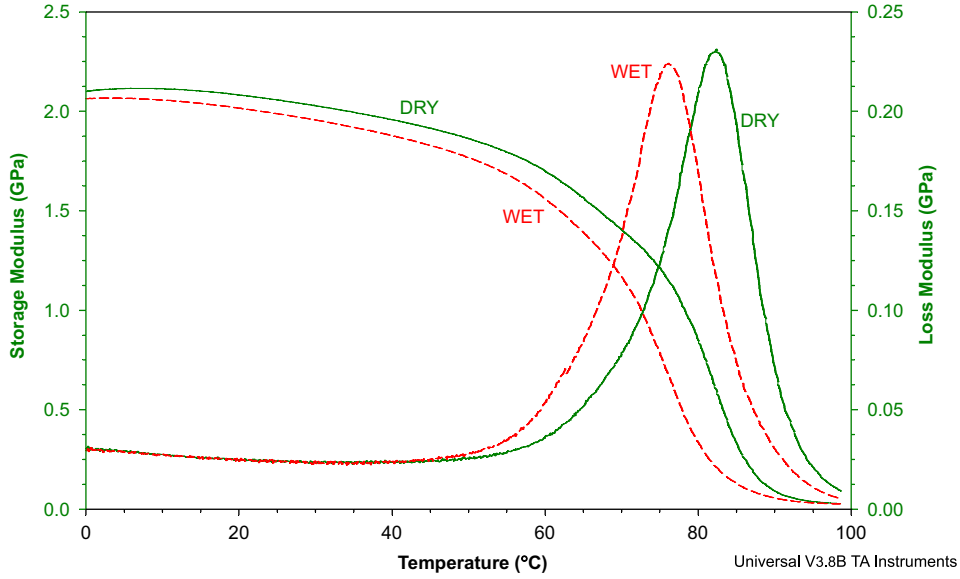

Fig. 7. Measurements of dynamic storage and loss moduli of specimens of the adhesive that have been stored dry and under ambient humidity.

As found earlier with the analysis of creep results from dry specimens, it is expected that the retardation time parameters τ and t_0 will decrease with stress giving rise to non-linear creep. This creep function has been used to model the creep results shown in Fig. 5 for the adhesive with absorbed water and the resultant fits to the data are shown in Fig. 8. Values for the parameters in Eq. (14) used to obtain these fits are listed in Table 3. In determining these values, it has been assumed that ΔD, n and m do not change with stress. The broken lines with each curve in Fig. 8 are the contributions to the creep compliance at that stress from the short-time relaxation mechanism. It is apparent from this plot that the short-time process dominates creep behaviour at low stresses whilst, by virtue of the larger reduction in t_0 with increasing stress, the α-process dominates behaviour at high stresses.

The dependence of the mean retardation time parameters τ and t_0 in Table 3 on stress can be described by the same relationship given by Eq. (8) that was applied to the dry material in Fig. 3. This is demonstrated by the linear fits to plots of $\log_e t_0$ and $\log_e \tau$ against $(\text{stress})^2$ shown in Fig. 9. New parameters B and β are defined such that

$$t_0 = A \exp -(\alpha\sigma^2),$$
$$\tau = B \exp -(\beta\sigma^2), \qquad (15)$$

From the results in Fig. 9, values for the parameters A, B, α and β in Eqs. (15) can be derived and are $A = 3.2 \times 10^{12}$ s, $B = 3.6 \times 10^{7}$ s, $\alpha = 0.021\,(\text{MPa})^{-2}$ and $\beta = 0.0062\ (\text{MPa})^{-2}$.

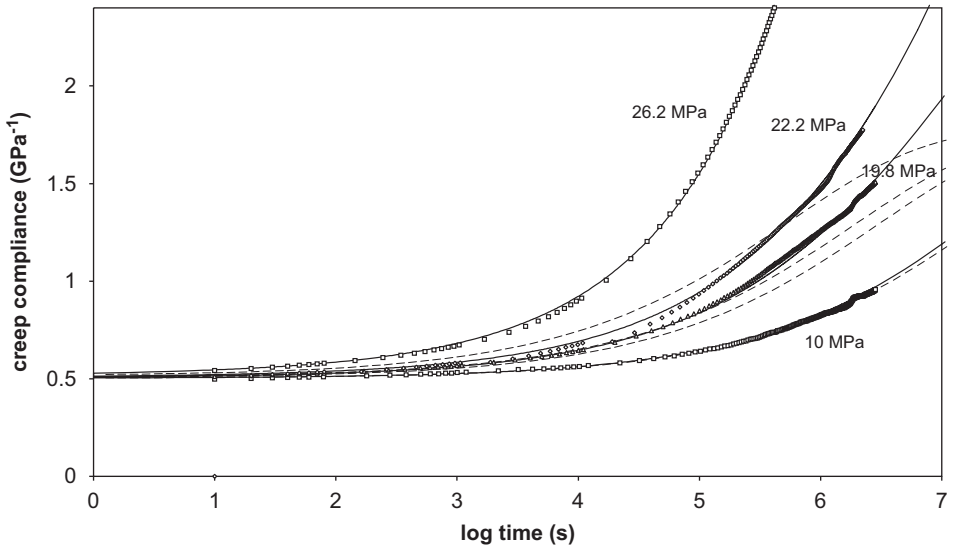

Fig. 8. Creep curves for the epoxy adhesive stored under ambient humidity. The continuous lines are best fits using Eq. (14). The broken lines are the calculated contributions from the short-time relaxation process.

Table 3
Values for the parameters in Eq. (14) used to obtain the fits to data in Fig. 8

σ_0	D_0 (GPa^{-1})	ΔD (GPa^{-1})	τ (s)	n	t_0 (s)	m
9.9	0.503	1.2	2×10^{7}	0.4	4.0×10^{11}	0.3
19.8	0.505	1.2	2.8×10^{6}	0.4	8.0×10^{8}	0.3
22.2	0.508	1.2	1.8×10^{6}	0.4	1.0×10^{8}	0.3
26.2	0.515	1.2	5×10^{5}	0.4	1.6×10^{6}	0.3

4.2. Compressive creep in the adhesive with absorbed water

Fig. 10 compares the results of creep tests on specimens of the adhesive with absorbed water under tension and compression at a stress of 26 MPa. As with results for the dry adhesive shown in Fig. 4, creep under compression is shifted to longer times compared with tension at the same stress. The fit to the compressive creep results in Fig. 10 has been obtained using the two-process creep function given by Eq. (14) assuming ΔD, n and m are the same for both tension and compression and therefore the only parameters to change are the retardation times τ and t_0.

Values for these parameters for the fits in Fig. 10 are shown in Table 4. Values for the other parameters are the same as those in Table 3. These increases in retardation times under compression can be modelled, as explained in Section 3.2, by assuming that retardation times are dependent upon the stress state as well as the stress magnitude. Eq. (15) must then be expressed in terms of effective stresses $\bar{\sigma}_1$ for the first process and $\bar{\sigma}_2$ for the second process in which case Eqs. (15) become

$$\tau = B\exp-\beta\bar{\sigma}_1^2,$$
$$t_0 = A\exp-\alpha\bar{\sigma}_2^2. \tag{16}$$

Following the analysis in Section 3.2, these effective stresses are given by the expressions

$$\bar{\sigma}_1 = \frac{(\lambda_1+1)}{2\lambda_1}\sigma_e + \frac{3(\lambda_1-1)}{2\lambda_1}\sigma_m,$$
$$\bar{\sigma}_2 = \frac{(\lambda_2+1)}{2\lambda_2}\sigma_e + \frac{3(\lambda_2-1)}{2\lambda_2}\sigma_m. \tag{17}$$

The values for τ and t_0 in Table 4 and for B, β, A and α in Fig. 8 allow the magnitudes of λ_1 and λ_2 to be calculated as $\lambda_1 = 1.1$ and $\lambda_2 = 1.2$.

5. A re-evaluation of creep in the dry adhesive

The analysis of creep results for the dry adhesive in Section 3 of this paper in terms of a single relaxation process model, although quite successful, did show signs of a consistent departure of the data from the model at elevated stresses. Furthermore, the values obtained for the retardation time parameter t_0 in Table 1 are significantly smaller than the values for t_0 for the second process recorded in Table 3 despite the T_g for the dry material being higher than that for the material with absorbed water. Whilst there is no clear evidence of two relaxation processes contributing to the creep behaviour of the dry material, it is possible that, in the absence of absorbed water, the amplitude ΔD of the first process may be smaller but still significant. To explore this possibility, the creep results in Fig. 2 for the dry material have been analysed using the two-process, creep function in Eq. (14). Results are shown in Fig. 11.

In obtaining these fits, it has been assumed that the magnitudes of the parameters n and m are the same in both materials and that the parameter ΔD is lower for the dry material but does not vary with stress. Values for the parameters in Eq. (14) used to obtain the fits to the data shown in Fig. 11 are recorded in Table 5.

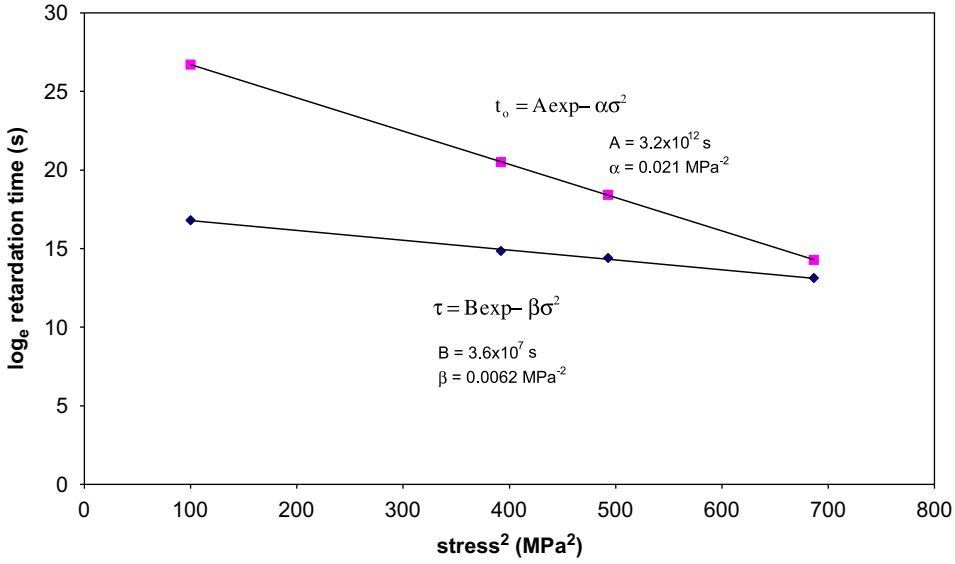

Fig. 9. Plots of $\log_e$ retardation times against the square of the creep stress obtained from the data fits in Fig. 8 (see Table 3).

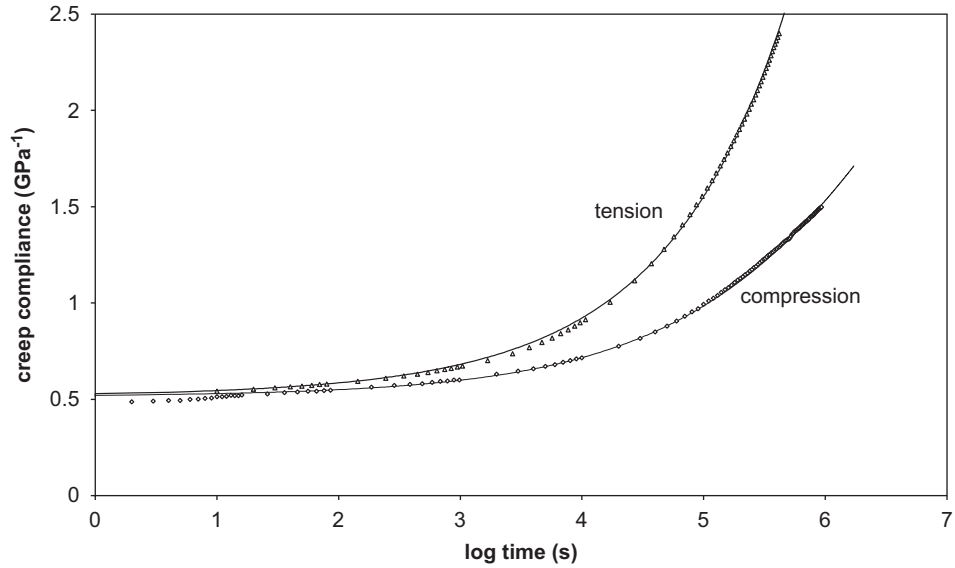

Fig. 10. Creep curves under tensile and compressive stresses of 26 MPa for the adhesive stored at ambient humidity. See Table 4 for retardation times obtained using the two-process model.

Table 4
Values for retardation time parameters under tension and compression at 26 MPa

Tension		Compression	
τ (s)	t_0 (s)	τ (s)	t_0 (s)
5×10^5	1.6×10^6	1.2×10^6	1.8×10^8

6. Discussion

The good fits to the creep data for adhesive specimens that have been stored at ambient humidity and for dry material in Figs. 8 and 11, respectively, have been obtained using a function (Eq. (14)) with six adjustable parameters. It is possibly not surprising, therefore, that good fits can be obtained. Despite this, the dependence on stress for each material is obtained with only two of the parameters, the retardation times, varying with stress. Because of the overlap in creep time of the two processes, there is little clear information on appropriate values for the amplitude ΔD of the first process. However, it should generally be possible, as explained in Section 4.1, to obtain good estimates from accurate values of dynamic modulus from dynamic mechanical measurements at temperatures above ambient. The determination of more confident values for this parameter and others in the two-process creep function might be more evident with other epoxy adhesives where the glass transition temperature is higher and the overlap is therefore less for the two relaxation processes.

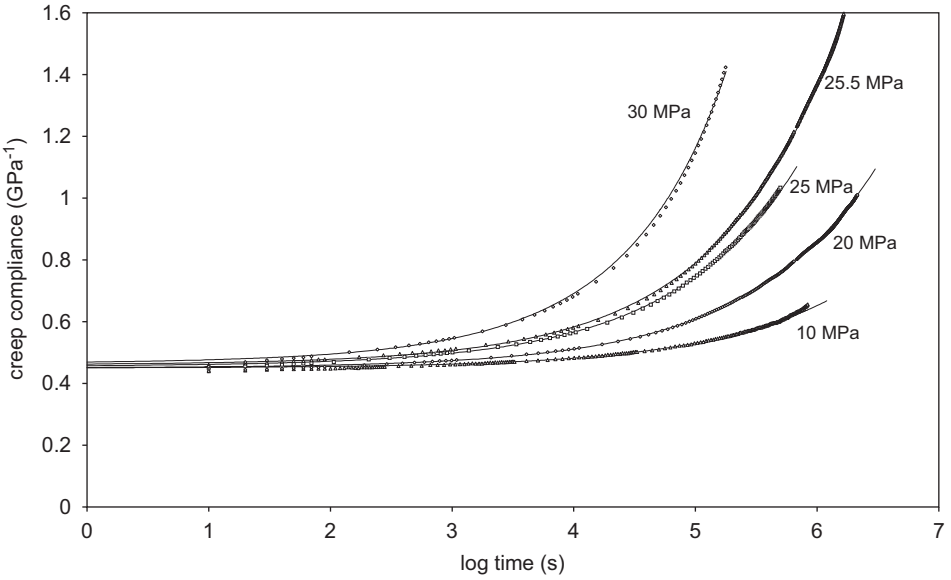

Fig. 11. Creep curves for the dry adhesive modelled using the two-process model.

Table 5
Values for the parameters in Eq. (14) used to obtain the fits to data in Fig. 11

σ_0 (MPa)	D_0 (GPa^{-1})	ΔD (GPa^{-1})	τ (s)	n	t_0 (s)	m
10	0.45	0.7	2.4×10^7	0.4	4×10^8	0.3
20	0.45	0.7	5×10^6	0.4	3×10^7	0.3
25	0.455	0.7	1.2×10^6	0.4	6×10^6	0.3
25.5	0.46	0.7	1.0×10^6	0.4	3×10^6	0.3
30	0.465	0.7	3.2×10^5	0.4	2.5×10^5	0.3

This uncertainty in the determination of parameter values that support the two-process model implies that alternative explanations for creep behaviour in this epoxy should be explored. The creep deformation could involve a single relaxation process for which the distribution of retardation times of the molecular motions comprising the process cannot be represented by a simple function with single parameters characterising a mean retardation time and a distribution of retardation times m.

The results shown here demonstrate the sensitivity of creep deformation of epoxy adhesives to even small quantities of absorbed water. This observation further complicates the analysis of creep measurements on dry material in the tests reported here since the humidity is not controlled during the creep test. For creep times greater than one or two weeks, the progressive increase in the concentration of absorbed water will influence the shape of a creep curve and hence the values of the parameters in the creep function used to model the creep deformation. This may explain the apparent anomaly in some of the values for the parameter t_0 for the wet and dry adhesive recorded in Tables 3 and 5. Since the presence of absorbed water in the adhesive lowers the glass transition temperature T_g, values for the retardation times τ and t_0 for the dry material, at a particular stress, are expected to be larger than values for the adhesive with absorbed water. Whilst this is true for the values for τ in Tables 3 and 5 and for t_0 at the higher stresses, it is not observed at stresses of 10 and 20 MPa. This could simply arise from a lack of precision in the determination of t_0 at these stress levels but the presence of small concentrations of water in the tests on the dry material could contribute significant errors, especially at low stresses where the contribution to the creep compliance from the second process only becomes significant at long creep times.

7. Conclusions

The creep behaviour of the two-part epoxy studied here can be modelled in the dry state by a simple, empirical function in which the range and population of retardation times in the creep relaxation process is represented by an effective (or mean) retardation time and a parameter that characterises the spectrum of retardation times.

Non-linear creep behaviour arises because the mean retardation time parameter is dependent on the magnitude of the creep stress. At elevated stresses where behaviour is non-linear, creep under uniaxial compression is significantly different from deformation under a tensile stress of the same magnitude implying that the retardation time parameter depends on the stress state as well as the stress magnitude. This has been modelled by an expression that relates the mean retardation time to the magnitudes of the shear and the hydrostatic components of the applied stress.

This simple model is however unable to describe creep deformation in the adhesive that has absorbed water through prolonged storage under ambient humidity. Some success has been achieved here by modelling the behaviour in terms of contributions from two relaxation mechanisms whose retardation time spectra overlap at moderate creep

times. This interpretation implies that the magnitude of the shorter retardation time process increases with the content of absorbed water, and this process therefore dominates the creep behaviour of the material with absorbed water at short creep times. Whilst the retardation times of both processes decrease with increasing stress, leading to non-linear creep, the decrease in the retardation time of the second, longer time process with stress is greater than that for the shorter time process. The creep deformation at higher stresses is thereby dominated by the second process.

There is evidence that the creep behaviour of the dry material is also composed of contributions from two processes. It is suggested that the contribution from the short-time process in dry material is smaller but not zero. When the creep behaviour of the dry material is analysed in terms of a two-process model, the fit to experimental data is better than achieved with the single-process model, and the values for the parameters for the dry material and the material with the absorbed water are more consistent.

Studies of non-linear creep in other epoxy resins and the influence of water on creep behaviour should provide further information on some of the issues raised in this paper.

Acknowledgements

The author would like to acknowledge the assistance of Mr. B. Sikkel at 3M Ltd with the supply of adhesive material, of Mr. R. Shaw at NPL with the preparation of specimens of the adhesive and of Dr. W. Broughton with helpful discussions of the work. The work was funded by the Department of Trade and Industry as part of the Performance Programme.

References

[1] Miyano Y, Nakada M, Kasamori M, Muki R. Mech Time-dependent Mater 2000;4:9.
[2] Feng C-W, Keong C-W, Hsueh Y-P, Wang Y-Y, Sue H-J. Int J Adhesion Adhesives 2005;25:427.
[3] Ponteins P, Medda B, Demont P, Chatain D, Lacabanne C. Poly Eng Sci 1997;37:1598.
[4] Hu Y, Xia Z, Ellyin F. Polym and Polym Composites 2000;8:11.
[5] Dean G, Crocker L, Read B, Wright L. Int J Adhesion Adhesives 2004;24:295.
[6] Popelar C, Liechti K. Mech Time-dependent Mater 2003;7:89.
[7] Williams G, Watts DC. Trans Faraday Soc 1970;66:80.
[8] Read BE, Dean GD, Tomlins PE. Polymer 1988;28:2159.
[9] Dean GD, Read BE, Tomlins PE. Plastics and rubber process. Appl 1990;13:37.
[10] Struik LCE. Physical aging in amorphous polymers and other materials. Amsterdam: Elsevier; 1978.
[11] Tomlins PE, Read BE, Dean GD. Polymer 1994;35:4376.
[12] Read BE. J Rheol 1992;36:1719.
[13] Dean GD, Tomlins PE, Read BE. Polym Engng Sci 1995;35:1282.
[14] Eyring HJ. Chem Phys 1936;4:283.
[15] Crist B. The physics of glassy polymers. In: Haward RN, Young RJ, editors. 2nd ed. London: Chapman & Hall; 1997 [chapter 4].
[16] Ward IM. In: Mechanical properties of solid polymers. 2nd ed. New York: Wiley; 1983 [chapter 11].
[17] Raghava R, Caddell RM, Yeh GS. J Mater Sci 1977;99:2.
[18] Wang J, Ploehn HJ. J Appl Polym Sci 1996;59:345.
[19] Colombini D, Martinez-Vega JJ, Merle G. Polymer 2002;43:4479.